

Visualization techniques for surface analysis

Stefanie Hahmann*

hahmann@imag.fr

published in *Visualization techniques for surface analysis*, in C. Bajaj (ed.): Advanced Visualization Techniques, John Wiley, (1999)

1.	Introduction	2
1.1	Purposes of surface interrogation	2
1.2	Overview	3
2.	Review of differential geometry	4
3.	Surface interrogation methods	7
3.1	Isolines	7
3.1.1	Contour lines	7
3.1.1	Parabolic lines	7
3.2	Light reflection methods	8
3.2.1	Reflection lines	8
3.2.2	Highlight lines	9
3.2.3	Isophotes	10
3.3	Variable surface offsets	13
3.3.1	Hedgehog diagrams and curvature plots	14
3.3.2	Generalized focal surfaces	15
3.4	Detection of inflections	18
3.4.1	Orthotomics	19
3.4.2	Polarity methods	19
3.5	Color mappings	20
3.5.1	Color maps	20
3.5.2	Pseudo texture	21
3.6	Characteristic lines	22
3.6.1	Lines of curvature, umbilics	22
3.6.2	Geodesic paths	23
4.	References	25

* Laboratoire LMC-IMAG, Université INPG Grenoble, BP 53, F-38041 Grenoble, France

Abstract. *Surface interrogation is of central importance for CAD and Computer Graphics applications. Wherever free form surfaces are used, they often need to be analyzed with respect to different aspects like, for example, visual pleasantness, technical smoothness, geometric constraints or surface intrinsic properties. The various methods, which are presented in this paper, can be used to detect surface imperfections, to analyze shapes or to visualize different forms.*

1. Introduction

The geometric modelling of free form curves and surfaces is of central importance for sophisticated CAD/CAM systems, for many computer graphics applications as well as in the field of numerical simulations based of finite element techniques. Surface interrogation methods find their origin in the CAD/CAM-technologies which require high quality surfaces. A wide variety of surface formulations have been developed to satisfy these requirements (see, for example, Böhm, Farin, Kahmann [6], Farin [13], Hoschek, Lasser [25] for an overview).

Surfaces in automobile design need to be smooth and need to have nice reflection characteristics. Ship hull design necessitates minimal energy surfaces. NC-processing has special requirements on surfaces. Milling machines limit the amount of curvature radii of the surface. The flow behaviour of surfaces in aerodynamic studies (turbine blade, air plane wings,...) depends on the continuity and smoothness of the underlying surface. A lot of other examples can be found in order to underline that surface interrogation is a key issue in the geometric design process.

1.1 Purposes of surface interrogation

Surface interrogation methods provide important tools in analyzing the intrinsic shape and curvature properties of parametric surfaces. They frequently reveal anomalous behaviour which is not immediately apparent in simple isoparametric curve digitizations or in high-resolution shaded images.

While defining parametric surfaces interpolatory or boundary constraints need to be satisfied (for example, fitting surfaces to arrays of discrete points, generation of blend surfaces). But they often introduce undesired surface behaviours due to the poor control over their many degrees of freedom. Analysis tools are needed for detecting such surface imperfections.

Most applications in industrial design require

- smoothness and
- shape fidelity.

The need of fair or smooth surface shapes can be motivated by different considerations. In automobile design aesthetic aspects are dominating, while in aircraft and ship design aerodynamics and hydrodynamic constraints must be satisfied.

The smoothness therefore is related to a lot of different surface features, like

- continuity between adjacent patches in tangents and curvature,
- curvature distribution,
- flat points,
- convexity,

which are driven directly from the surface differential geometry. Aesthetically smooth surfaces must not have

- bumps, dents (surface irregularities)

which can be described mathematically as small curvature variations. Smooth surfaces also need to have

- nice light reflection behaviour.

More technical considerations in surface design are NC milling verification, robot collision detection, and so on. The recognition of surface imperfections, like

- exceed of curvature bounds,
- high variation of curvature

can prevent failure of tool-path generation algorithms for example.

The detection of surface imperfections like those mentioned above is one task of surface interrogation methods. Some of them are surveyed in Hagen et al. [18]. Another application, not necessarily disjoint from the first one, is the visualization of differential geometry surface features like

- curvature behaviour (principal curvature, Gaussian curvature),
- parabolic lines,
- isolines
- lines of curvature
- umbilics,
- geodesic lines.

They provide tools for a detailed analysis of the intrinsic geometry of the surface with various applications and they facilitate the design of surfaces (see, for example, Beck et al. [2]).

1.2 Overview

The main purpose of this chapter is to give an overview of surface interrogation methods. Due to the large number of different applications of surface interrogation one feels tempted to divide these techniques into two main subgroups: techniques for *visualizing surface features* and techniques for *detecting and remedying unexpected surface characteristics*. But there are some methods, like isoline ex., which thwart this plan because they belong to both groups. On one hand they are used to visualize surface features, to increase the 3D-understanding, to analyze the intrinsic geometry of the surface and on the other hand they interrogate the smoothness/fairness of surfaces and their technical suitability for NC processing. Various visualization techniques identify unwanted surface features, but no method is optimal for all applications.

In order to keep the reader free in its choice of the appropriate surface interrogation method for a specific application, the chapter will be structured as follows: Before we

turn to a detailed presentation of surface analysis techniques, we will briefly give a review of differential geometry (section 2). In Sect.3 the presentation of each surface interrogation method is accompanied by examples of applications.

2. Review of differential geometry

The differential geometry of surfaces is fundamental for the following sections. There are many literature on this subject (DoCarmo [10], Eisenhart [11], Kreyszig [29], Böhm [5]), so we only summarize the relevant definitions here.

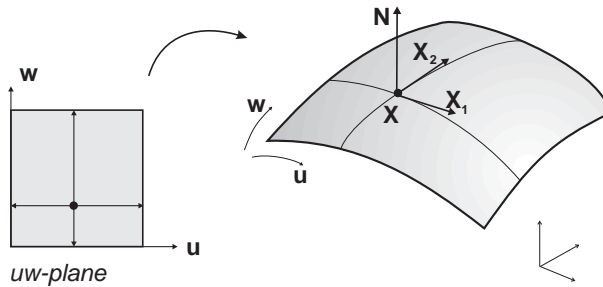


Figure 1: *Parametric surface*

Let us consider a surface in real euclidean 3-space \mathbb{R}^3 , given in parametric representation

$$X = X(u, w) = \begin{bmatrix} x(u, w) \\ y(u, w) \\ z(u, w) \end{bmatrix}, \quad (u, w) \in G \subset \mathbb{R}^2, \quad (2.1)$$

where $X \in C^r(G)$. To avoid undefined normal vectors, we assume a regular parameterization, i.e., the partial derivative vectors $X_1 := \frac{\partial X}{\partial u}$, $X_2 := \frac{\partial X}{\partial w}$ are linear independent in G . The unit normal vector of $X(u, w)$ can then be defined as

$$N(u, w) := \frac{X_1 \times X_2}{\|X_1 \times X_2\|}, \quad (2.2)$$

where \times denotes the cross product. There are two important geometric structures defined by the surface which completely characterize the shape of the surface: the first and second fundamental forms.

The two fundamental forms: The *first fundamental form* I is also called metric form, because it allows to make measurements on the surface like lengths, areas and angles between two curves on the surface. A regular curve $[u(t), w(t)]^T$ in the uw -plane defines a regular curve $X(u(t), w(t))$ on the surface.

The (squared) arc element of this curve is then given by

$$ds^2 = dX \cdot dX = g_{11}du^2 + 2g_{12}dudw + g_{22}dw^2, \quad (2.3)$$

where $g_{ij} = X_i \cdot X_j$, ($i, j = 1, 2$), and is called *first fundamental form* $I := ds^2$. The subscripts denote partial derivatives. The arc element ds is a geometric invariant, i.e.,

does not depend on the particular parameterization chosen for the representation (2.1) of the surface.

While the first fundamental form I is defined as the dot product of the infinitesimal displacement of any curve on the surface dX by itself, the *second fundamental form* II is defined as the dot product of dX of any surface curve and infinitesimal variation dN of the surface unit normal N along such a curve:

$$II = -dX \cdot dN = h_{11}du^2 + 2h_{12}dudw + h_{22}dw^2, \quad (2.4)$$

with $h_{ij} = -X_i \cdot N_j = X_{ij} \cdot N$, $i, j = 1, 2$. The second fundamental form II together with the first fundamental form I allows to compute the surface curvatures.

Surface curvatures: The family of planes containing the surface normal N at a given point P cuts the surface in a family of *normal section curves* C for that point.

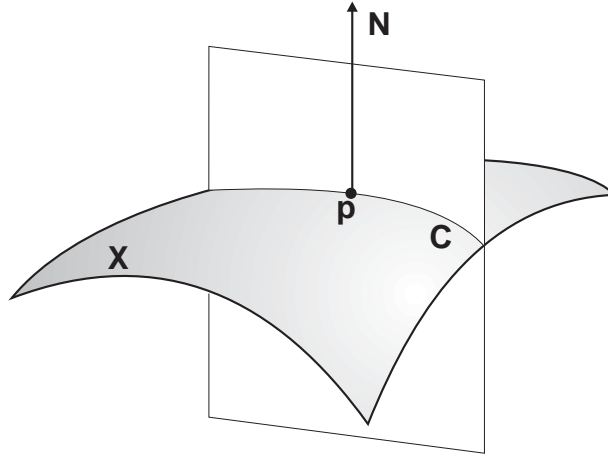


Figure 2: Normal section curve

Let \mathbf{t} be the tangent vector of the normal section curve C at P . The *normal curvature* κ of the surface is defined as the curvature of the normal section curve and can be calculated by utilizing differentiation of equation $N \cdot \mathbf{t} = 0$ along C with respect to arc length:

$$\kappa = \kappa(\lambda) = -\frac{d\mathbf{t}}{ds} \cdot N = \mathbf{t} \cdot \frac{dN}{ds} = \frac{dX}{ds} \cdot \frac{dN}{ds} = -\frac{II}{I} = -\frac{h_{11} + 2h_{12}\lambda + h_{22}\lambda^2}{g_{11} + 2g_{12}\lambda + g_{22}\lambda^2}, \quad (2.5)$$

where $\lambda = dw/du$ specifies the direction of the curve, see figure 2. The negative sign in equation (2.5) gives positive curvature if the center of curvature lies opposite to the direction of the surface normal (convex). In the special case where $g_{11} : g_{12} : g_{22} = h_{11} : h_{12} : h_{22}$, the normal curvature κ is independent of λ . Points with that property are called *umbilical points*.

In general, at each point κ varies with each direction $\lambda = dw/du$. The extreme values κ_1 and κ_2 of $\kappa(\lambda)$ occur at the roots λ_1 and λ_2 of

$$\det \begin{vmatrix} \lambda^2 & \lambda & 1 \\ g_{11} & g_{12} & g_{22} \\ h_{11} & h_{12} & h_{22} \end{vmatrix} = 0. \quad (2.6)$$

The extreme values κ_1 and κ_2 satisfy the two simultaneous equations

$$\begin{aligned}(h_{11} + \kappa g_{11})du + (h_{12} + \kappa g_{12})dw &= 0 \\ (h_{12} + \kappa g_{12})du + (h_{22} + \kappa g_{22})dw &= 0,\end{aligned}\tag{2.7}$$

and are therefore the roots of

$$\det \begin{vmatrix} \kappa g_{11} - h_{11} & \kappa g_{12} - h_{12} \\ \kappa g_{12} - h_{12} & \kappa g_{22} - h_{22} \end{vmatrix} = 0.\tag{2.8}$$

κ_1 and κ_2 are called *principal curvatures* ($\kappa_1 = \kappa_{\max}$, $\kappa_2 = \kappa_{\min}$). The corresponding directions λ_1, λ_2 define directions in the uw -plane and the corresponding directions in the tangent plane are called *principal curvature directions*. They are always orthogonal except at umbilical points ($\kappa_1 = \kappa_2$) where the principal directions are undefined. A special umbilical point is a *flat point* ($\kappa_1 = \kappa_2 = 0$) where the surface becomes locally flat. Umbilical points are also called spherical points, since the surface locally approximates a sphere at those points.

The net of lines that have the principal directions at all their points is called net of *lines of curvature*. It can be calculated by integrating equations (2.7).

Gaussian and mean curvature: The two principal curvatures κ_1 and κ_2 are given by

$$\begin{aligned}\kappa_1 &= H + \sqrt{H^2 - K} \\ \kappa_2 &= H - \sqrt{H^2 - K},\end{aligned}\tag{2.9}$$

where K is the *Gaussian curvature* and H is the *mean curvature*. They are defined by

$$\begin{aligned}K &= \frac{h_{11}h_{22} - h_{12}^2}{g_{11}g_{22} - g_{12}^2} \\ H &= \frac{2g_{12}h_{12} - g_{11}h_{22} - g_{22}h_{11}}{2(g_{11}g_{22} - g_{12}^2)}.\end{aligned}\tag{2.10}$$

From (2.9) follows that

$$\begin{aligned}K &= \kappa_1\kappa_2 \\ H &= \frac{\kappa_1 + \kappa_2}{2}.\end{aligned}\tag{2.12}$$

If κ_1 and κ_2 are of the same sign, i.e., if $K > 0$, the point under consideration is called *elliptic* (for example: ellipsoid). If κ_1 and κ_2 have different signs, i.e., if $K < 0$, the surface point is called *hyperbolic*. If either κ_1 or κ_2 is zero, the Gaussian curvature is zero and the surface point is called *parabolic*.

3. Surface interrogation methods

3.1 Isolines

Isolines are an interrogation tool with a wide variety of applications. They provide powerful intuition in understanding curved surfaces. They help analyzing surface characteristics and they are used to visualize the distribution of scalar quantities over the surface. Isolines are lines of a constant characteristic value on the surface. The visualization of a certain number of isolines, with respect to an even distribution of the characteristic values allows to study the behaviour of these values.

3.1.1 Contour lines

Contour lines are planar lines on the surface which are all parallel to a fixed reference plane. Closed contour lines indicate maxima and minima of the surface with respect to the direction given by the plane's normal vector (see Hartwig, Nowacki [20], or Beck, Farouki, Hinds [2]). Saddle points appear as “passes”. The contour lines only cross in the exceptional case of a contour at the precise level of a saddle point. Nackman [35] describes systematically the distribution of other critical points on a surface. A disadvantage of contour lines is the fact that they are costly to compute. Several surface contouring methods exist, which are sometimes depending of the specific surface formulation (see Petersen [36], Scatterfield, Rogers [40], Lee, Fredericks [30]). Hartwig and Nowacki [20] propose to subdivide the surface into sufficient small pieces which are then approximated by bilinear surfaces. Then the contour lines can easily be computed.

3.1.2 Parabolic lines

Parabolic lines are mentioned here as an example for isolines of a constant function value over the surface. Parabolic lines are lines of zero Gaussian curvature on the surface. They divide the surface into elliptic and hyperbolic regions and they reflect therefore the local curvature behaviour of a surface. Parabolic lines are special Gaussian curvature lines.

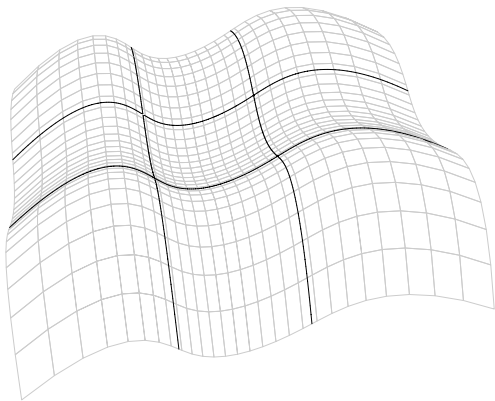


Figure 3a: *Parabolic lines*

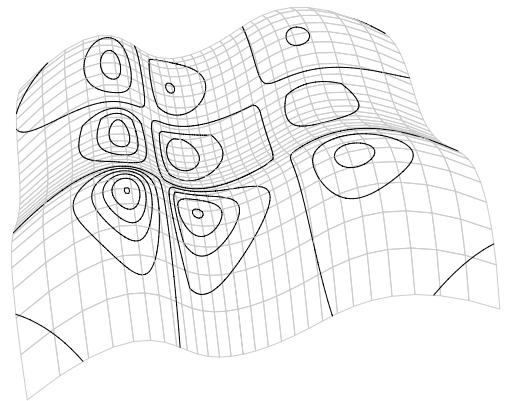


Figure 3b: *Gaussian curvature isolines*

The idea of plotting parabolic lines is not new. As reported by Hilbert and Cohen-Vossen [22], Felix Klein speculated that the artistic beauty of the statue Apollo Belvedere “...

was based on certain mathematical relations...”. But he couldn’t discover any general law confirming his thesis.

Nevertheless Gaussian isolines plotted on an engineering surface give the designer insight in shape and can detect unwanted curvature behaviour, like changes in the sign of the Gaussian curvature.

3.2 Light reflection methods

The light reflection methods all simulate the special reflection behaviour of light sources or light lines on the surface. Due to the intuitive understanding that everybody has when he observes light reflections, these methods are very effective in detecting surface irregularities. They are therefore very well suitable for testing the fairness of surfaces. Because the surface normals are involved in the computation of these lines, they also can be used to visualize first order discontinuities, like tangent discontinuities.

3.2.1 Reflection lines

The reflection line method determines unwanted dents by emphasizing irregularities in the reflection line pattern of parallel light lines.

Let $X(u, w)$ be a representation of the surface to investigate, and let $N(u, w)$ be the unit normal vector of the surface. Furthermore a *light line* L is given in parameter form:

$$L(t) = L_0 + t \cdot \vec{s}$$

where $t \in \mathbb{R}$, and point A is a fixed eye point.

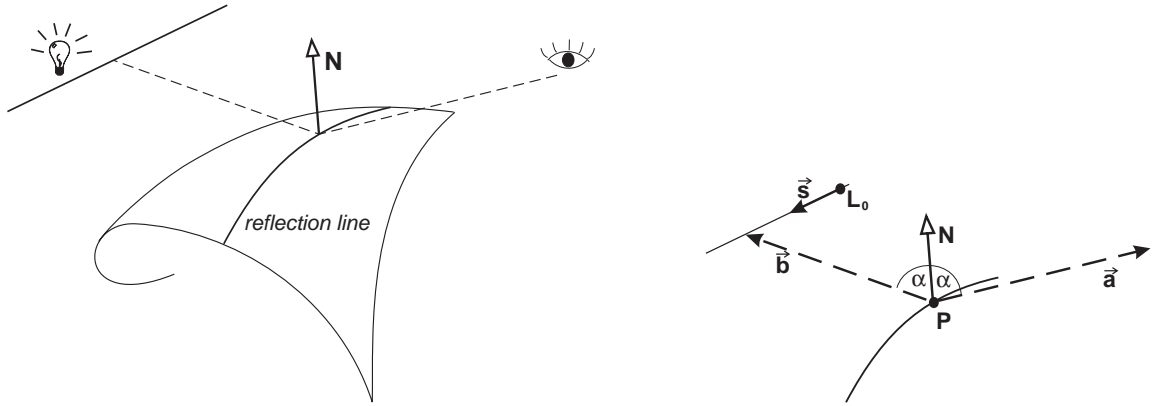


Figure 4: Reflection line method

The reflection line is the projection of the line L on the surface X , which can be seen from the eye point A , if the light line L is reflected on the surface, see figure 4.

From geometric dependencies the following reflection condition is easily seen:

$$\begin{aligned} \frac{\vec{a}}{\|\vec{a}\|} + \frac{\vec{b}}{\|\vec{b}\|} &= 2 \left(N(u, w) \cdot \frac{\vec{b}}{\|\vec{b}\|} \right) N(u, w) \\ &= 2 \left(N(u, w) \cdot \frac{\vec{a}}{\|\vec{a}\|} \right) N(u, w) \end{aligned}$$

where $\vec{a} = P - A$, $\vec{b} = L - P$. To evaluate the surface we use a set of reflection lines with direction \vec{s} and step along each curve of the set. For a fixed eye point A , the following non-linear system of equations for the unknown parameters u and w of the reflection point P has to be determined:

$$\vec{b} + \lambda \vec{a} = 2 \left(N(u, w) \cdot \vec{b} \right) N(u, w) \quad \text{with} \quad \lambda := \frac{\|\vec{b}\|}{\|\vec{a}\|}$$

These three non-linear equations can be reduced to two by eliminating λ ; this system can then be solved by numerical methods, but the existence and unambiguity of solutions has to be ensured by an appropriate choice of the eye point A (see Klass [28], [26]). Figure 5 shows a reflection line pattern on a part of a hair dryer and visualizes some surface irregularities.

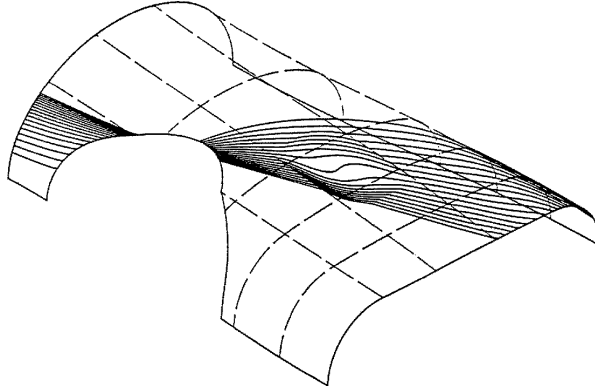


Figure 5: Reflection line analysis of a hair dryer

3.2.2 Highlight lines

The highlight line method also detects surface irregularities and tangent discontinuities by visualizing special light reflections on the surface. In comparison with the reflection line method, the highlight lines are calculated independently from any observers view point.

A highlight line is defined as the loci of all points on the surface where the distance between the surface normal and the light line is zero. The linear light source idealized by a straight line with an infinite extension

$$L(t) = L_0 + Bt$$

(A is a point on L , B is a vector defining the direction of L , $t \in \mathbb{R}$), is positioned above the surface under consideration. For a given surface point $X(u, w)$ let $N(u, w)$ be the unit normal vector. The surface point $X(u, w)$ belongs to the highlight line if both lines, $L(t)$ and the extended surface normal

$$E(s) = X(u, w) + s \cdot N(u, w), \quad s \in \mathbb{R}$$

intersect, i.e. if the perpendicular distance

$$d = \frac{\| [B \times N] \cdot [L_0 - X] \|}{\| [B \times N] \|}$$

between both lines is zero, see figure 6.

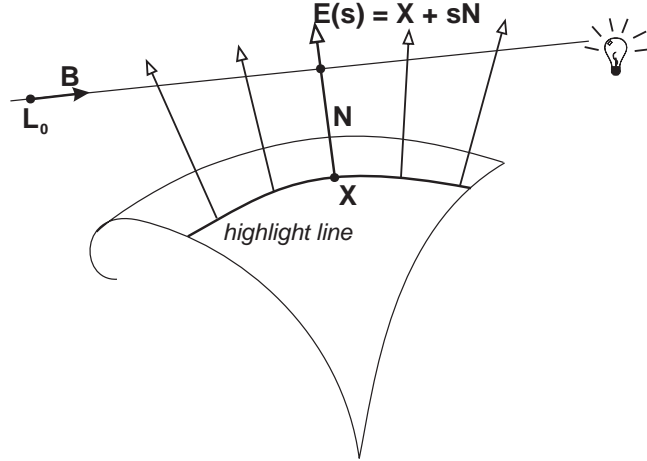


Figure 6: *Highlight line model*

This method can be extended to highlight bands, lines where $d \leq r$ (r fixed) is verified. For details on the algorithms to compute highlight lines, see Beier [3].

3.2.3 Isophotes

Classical Isophotes: This method analyzes surfaces by lines of equal light intensity, the isophotes. If $X(u, w)$ is a parameterization of the surface and L the direction of a parallel lighting, then the isophote condition is given by:

$$N(u, w) \cdot L = c, \quad (*)$$

where $c \in \mathbb{R}$ is fixed, see figure 7. Note that silhouettes are special isophotes ($c = 0$) with respect to the light source.

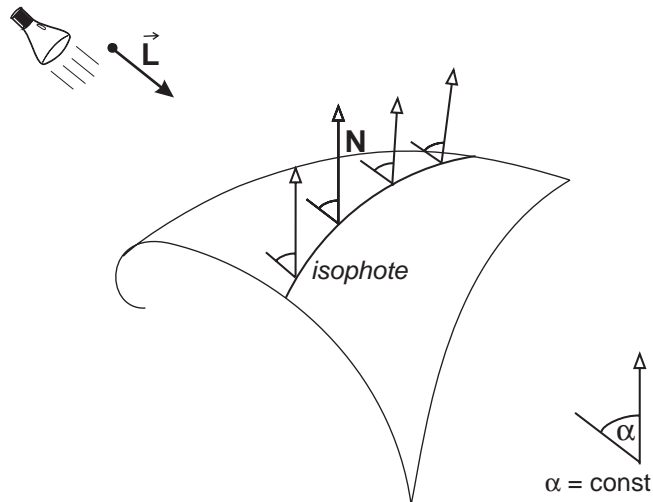


Figure 7: *Isophote method*

In the same sense as reflection lines and highlight lines, the isophotes provide a powerful tool to visualize small surface irregularities, which can't be seen with a simple wire frame or a shaded surface image. In figure 8 we use ten different values for c in order to get an isophote pattern on a test surface (left image). Fig. 8b and 8c then differ in a different choice of the light direction L .

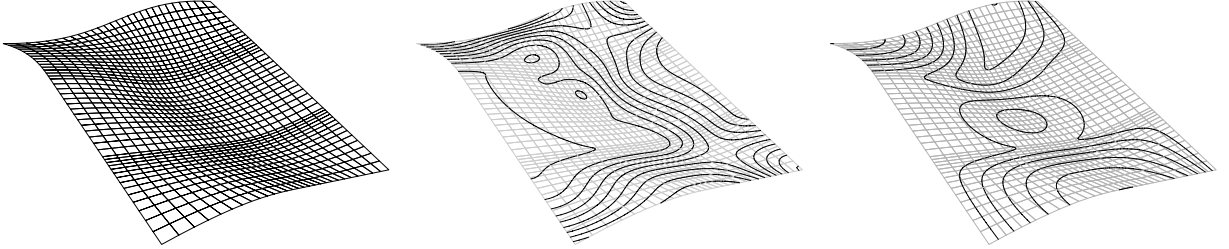


Figure 8a: *Test surface*

Figure 8b,c: *Analysis with isophotes*

Now, as stated out in the introduction of this section, the light reflection methods can be used to visualize first and second order discontinuities, because the surface normal vector is always involved in the line definitions. We will illustrate this property by using isophotes, for which the following statement holds: *If the surface is C^r -continuous, then the isophotes are C^{r-1} -continuous curves* (see for more details Poeschl [37]). Fig. 9a,c show surfaces displayed as a curve network which don't seem to have discontinuities across the boundaries of their patches. The isophotes on the other hand are discontinuous (gaps) at points where the surface is only C^0 across the boundary of the two patches.

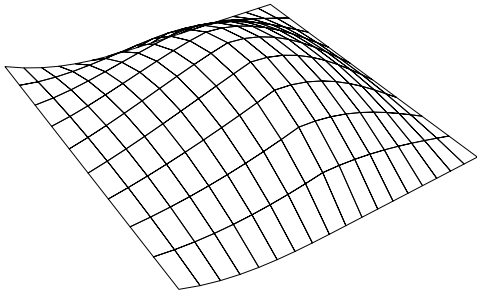


Figure 9a: *C^0 -continuous surface*

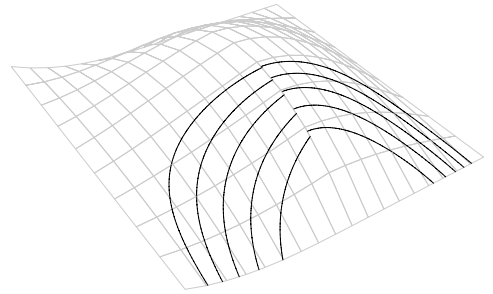


Figure 9b: *Analysis with isophotes*

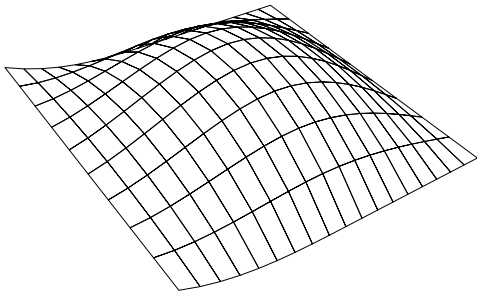


Figure 9c: *C^1 -continuous surface*

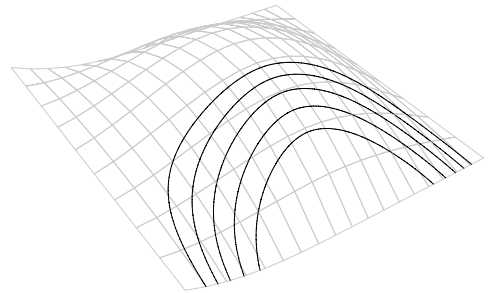


Figure 9d: *Analysis with isophotes*

A curvature discontinuity can be recognized, where the isophotes possess tangent discontinuities (breaks). Isophotes are constructed with the isophote conditions, whereby in general various different values for c are tested. The equations of type (*) are solved numerically.

One should nevertheless be careful by using isophotes for this purpose, because sometimes the break points of the isophotes at curvature discontinuities may not be clearly recognized, because of an ill-conditioned light direction. This is the case in figure 9d. Either the surface must be rotated, or the light direction must be changed. This special case occurs if the orthogonal projection of the light direction L in the tangent plane at a boundary point $X(u, w)$ is parallel to the tangent of the isophote at this point.

Isophotes for curvature discontinuity: There is another isophote method, which on one hand is an automatic method (independent of a special light direction), but which on the other hand only visualizes curvature discontinuities across the boundaries of a patch work. We give a short description of this algorithm, for the necessary fundamentals of differential geometry, see section 2.

The envelope of the tangent planes along a surface-curve y is a developable, ruled surface Φ . At each point p of y , the tangent \dot{y} is a conjugate to the corresponding ruling of Φ . Conjugate directions are conjugate diameters of the Dupin indicatrix. Such conjugate directions satisfy the symmetric bilinear equation:

$$h_{11}\Delta u\Delta\tilde{u} + h_{12}(\Delta u\Delta\tilde{w} + \Delta\tilde{u}\Delta w) + h_{22}\Delta w\Delta\tilde{w} = 0.$$

This relation degenerates at parabolic points, because the asymptotic direction (the direction in which the normal section curvature vanishes) is the conjugate to itself, but also conjugate to all other directions. At planar points, we have this degeneration for each (tangent) direction. Let X_1 and X_2 denote the two G^2 surface patches of the patchwork X , G^1 -continuously linked together along the common G^2 boundary curve y . Since both X_1 and X_2 have y as a surface curve, and the tangent planes along y are unique, the Dupin indicatrices i_1, i_2 have a common diameter, but in general there are no further common elements.

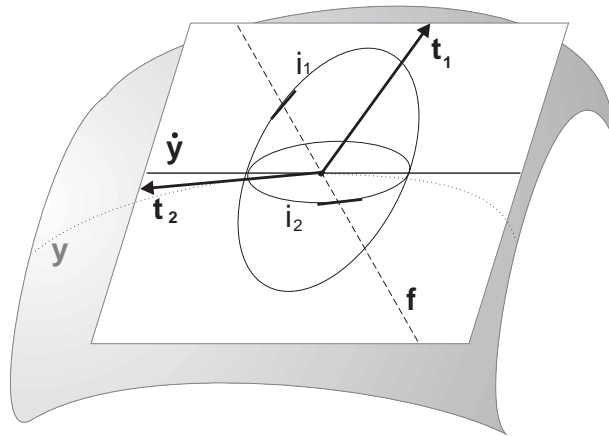


Figure 10: *Generalized isophote method*

We now consider an isophote c passing through P . The tangent t_i of c at P with respect to X_i is conjugate to the orthogonal projection f of the light ray onto the tangent plane ($i = 1, 2$), see figure 10. In general the isophote c shows a tangent discontinuity at P if the Dupin indicatrices of X_1 and X_2 are not equal, but we have to avoid the situations $f = \dot{y} = t$ and $f = t'$. These considerations lead to the following algorithm for displaying the curvature situation across the boundary curves of a patchwork surface:

1. step: give f
2. step: calculate the conjugate directions t_1 and t_2
and the angle α between t_1 and t_2
3. step: vary $f(\Delta u = \cos \varphi; \Delta w = \sin \varphi)$
and calculate α_{\max}
4. step: **if** $\alpha_{\max} = \pi$
 then the surface is G^2 -continuous
 else display curvature discontinuity

More details about this algorithm can be found in Pottmann [39]. Fig. 11a,b show the result for G^1 and G^2 -continuous surfaces.

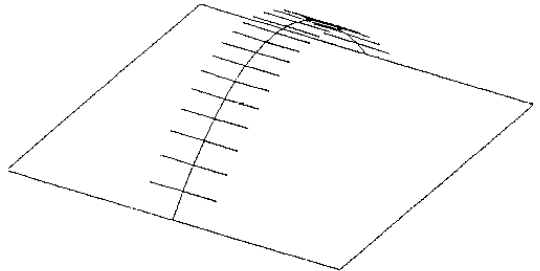
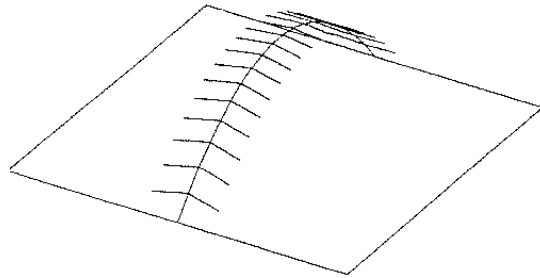
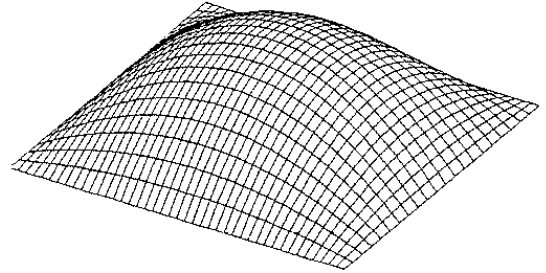
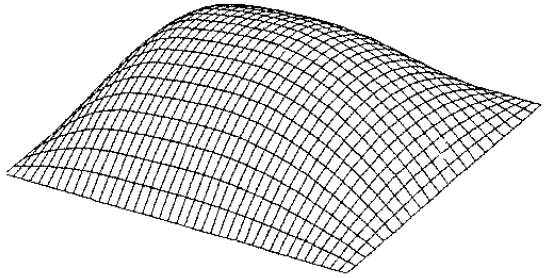


Figure 11a: G^1 -continuous surface

Figure 11b: G^2 -continuous surface

3.3 Variable surface offsets

Surface curvature is of central importance for surface design. Often the result must be mathematically smooth (continuous in the 2nd derivative) and aesthetically pleasing, i.e. have smooth flowing highlights and shadows. To obtain an aesthetically pleasing shape, the designer works with the curvature. A color map (see section 3.5) can be used to visualize curvature (Gaussian, principal curvatures) over the surface. The problem is

the good choice of the color scale, which depends on the curvature function and therefore of the underlying surface.

The surface interrogation methods presented in this section are therefore *curvature analysis* tools which are able to detect all surface imperfections related to curvature, like bumps, curvature discontinuity, convexity, and so on.

3.3.1 Hedgehog diagrams and curvature plots

The hedgehog diagrams and curvature plots are well known interrogation tools for planar curves (see, for example, Beier [3], Farin, Sapidis [14]). A hedgehog diagram for planar curves visualizes the curve normals proportional to the curvature value at some curve points. A new curve is obtained by $X_{hedgehog}(t) = X(t) + \kappa N(t)$.

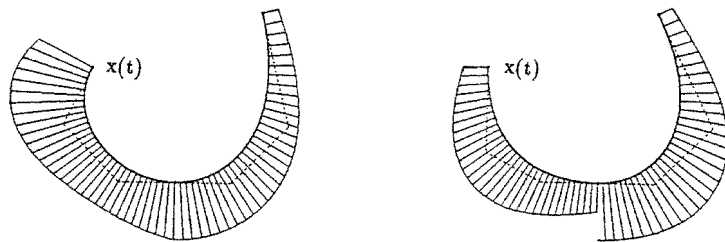


Figure 12: *Hedgehog diagram*

The inspection of surfaces with these methods can be done by applying them to planar curves on the surface (intersections of the surface with planes). Kjellander [27] shows an example of application.

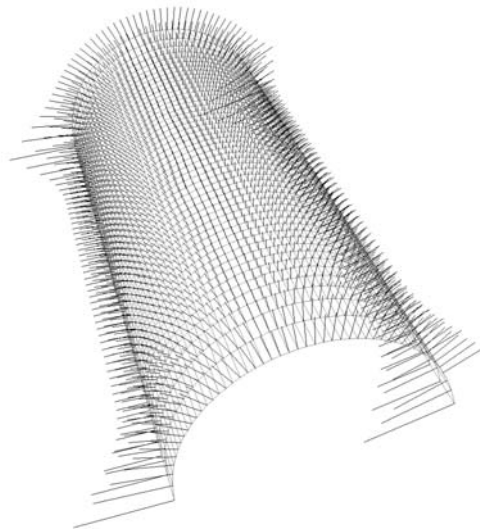


Figure 13: *Hedgehog diagram for surfaces*

Hedgehog diagrams for entire surfaces are difficult to interpret and are therefore not to be recommended.

3.3.2 Generalized focal surfaces

The idea of generalized focal surfaces is quite related to hedgehog diagrams. In stead of drawing surface normals proportional to a function value, only the point on the surface normal proportional to the function is drawn. The loci of all these points is the *generalized focal surface*. This method was introduced by Hagen and Hahmann [17], [19], and is based on the concept of focal surfaces which are known from line geometry. The focal surfaces are the loci of all focal points of an special line congruence, the normal congruence.

Given a set of unit vectors $E(u, w)$ one defines a *line congruence*:

$$C(u, w) = X(u, w) + D(u, w)E(u, w),$$

where $D(u, w)$ is called the signed distance between $X(u, w)$ and $E(u, w)$. If $E(u, w) = N(u, w)$, then C is a normal congruence. A *focal surface* $C_F(u, w)$ is a special normal congruence with $D(u, w) = \kappa_1^{-1}(u, w)$ or $D(u, w) = \kappa_2^{-1}(u, w)$:

$$C_F(u, w) = X(u, w) + \kappa_i^{-1}(u, w)N(u, w), \quad i = 1, 2$$

The generalization of this classical concept leads to the *generalized focal surfaces*:

$$F(u, w) = X(u, w) + s f(\kappa_1, \kappa_2) N(u, w), \quad \text{with } s \in \mathbb{R}$$

where N is the unit normal vector of the surface X . f is a real valued function in the parameter values (u, w) , see figure 14.

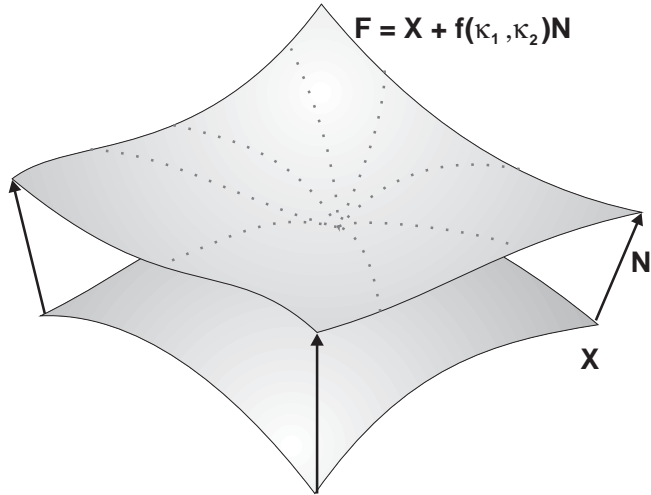


Figure 14: *Generalized focal surface construction*

The factor function f can be any arbitrary scalar function, but in the context of surface interrogation it is recommended to take f as a function depending on the principal curvatures κ_1, κ_2 of X .

variable offset functions:

- $f = \kappa_1 \kappa_2$ Gaussian curvature
- $f = 1/2(\kappa_1 + \kappa_2)$ mean curvature
- $f = (\kappa_1^2 + \kappa_2^2)$ energy functional
- $f = |\kappa_1| + |\kappa_2|$ absolute curvature
- $f = \kappa_i$ principal curvatures
- $f = \frac{1}{\kappa_i}$ focal points
- $f = \text{const}$ offset surfaces

Independent from the special choice of the offset function, the generalized focal surfaces F have the following properties:

- 2nd order surface interrogation method: $X \in C^n \Rightarrow F \in C^{n-2}$
- pin point property
- zoom property: s allows to zoom in or out a surface region of interest
- fast computation: point wise evaluation of 2nd and 3rd order derivatives.

The different offset functions listed below can now be used to interrogate and visualize surfaces with respect to the following criteria:

- convexity test
- detection of flat points
- detection of surface irregularities
- visualization of curvature behaviour
- visualization of technical smoothness
- visualization of C^2 - and C^3 -discontinuities
- test of technical aspects

Examples of application

- It is the only method which is able to detect *flat points*. A flat point is a special umbilic point, with $\kappa_1 = \kappa_2 = 0$. They are undesired surface points because they make the surface bumpy. The detection of flat points can be done by choosing one of the offset functions:

$$f = |\kappa_1| + |\kappa_2|$$

$$f = \kappa_1^2 + \kappa_2^2 .$$

A flat point occurs where both surfaces touch.

- *convexity test*: A surface is locally convex at $X(u, w)$, if the Gaussian curvature is positive at this point. Often a surface is called non convex, if there is a change in the sign of the Gaussian curvature. If one takes the offset function

$$f = \kappa_1 \cdot \kappa_2 = K ,$$

the two surfaces $X(u, w)$ and $F(u, w)$ intersect at the parabolic points. An example is shown in figure 15. The generalized focal surface therefore pin points directly on the area where the sign of K changes.

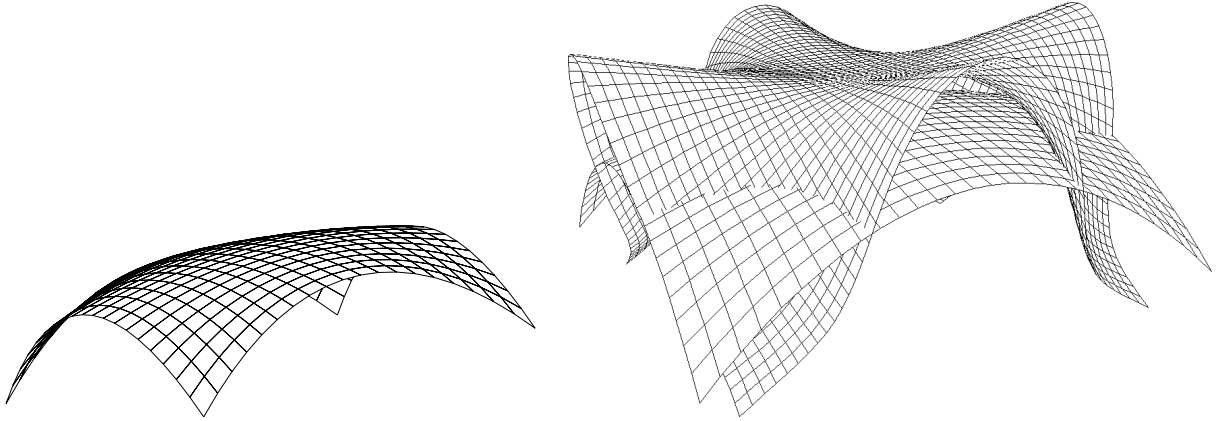


Figure 15: Convexity test with generalized focal surfaces

Orthotomics (see section 3.4.1) which are also used to test the convexity, don't pin point on the surface area where the problem arrives.

Generalized focal surfaces not only visualize surface imperfections, they also give the user a 3D impression of the relative amount of the offset function over the surface, what color maps can't do.

- *mathematical smoothness:* By using the offset function

$$f = \kappa_1^2 + \kappa_2^2,$$

the discontinuities of the second or third derivatives can be visualized by the generalized focal surfaces which are only C^{-1} or C^0 there.

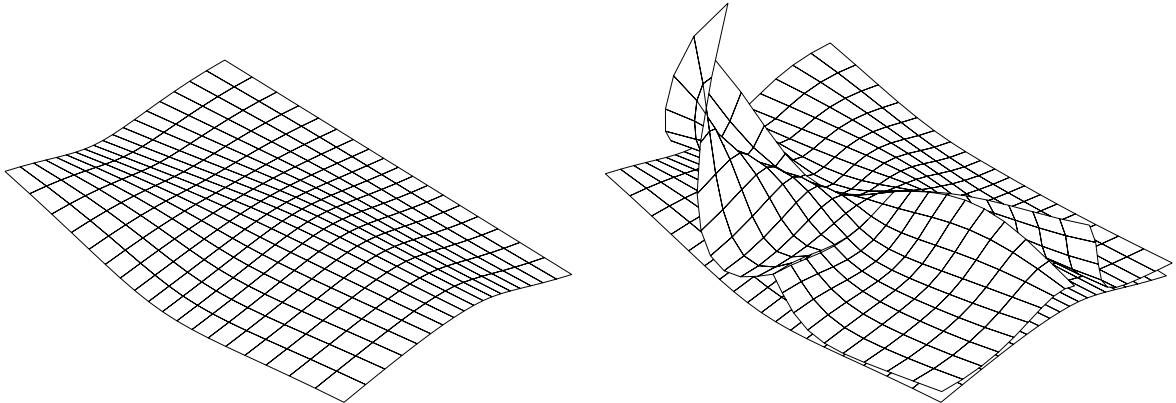


Figure 16: 4 bicubic patches: curvature discontinuity

- *visualizing technical aspects:* A surface which should be treated by a spherical cutter is not allowed to have a curvature radius smaller than the radius of the cutter R_{cutter} . The generalized focal surfaces are able to detect such undesired regions by intersection with the surface X . The offset function to choose in this special case, is

$$f = \frac{1}{R_{cutter}} - \kappa_{max}.$$

Fig. 17 shows such a surface which is not allowed to be cutted.

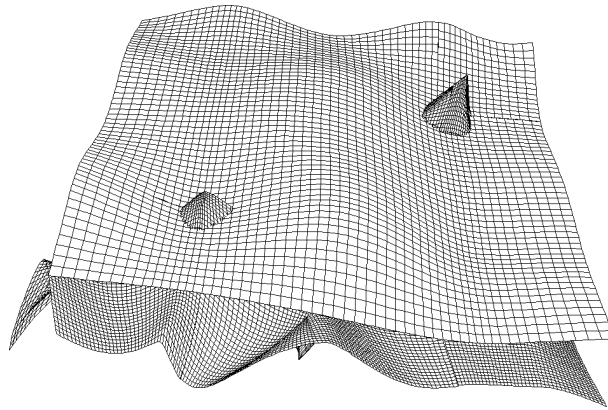


Figure 17: *Milling test*

- *visualizing surface irregularities:* Surfaces are aesthetically pleasing if they have “nice” light reflections. The reflection line methods visualize this property. The generalized focal surfaces are also a tool for visualizing such surface imperfections because they are very sensitive to small irregularities in the shape. In Fig. 18 parts of a hair dryer are shown. they consist of biquintic C^1 -continuous patches. The iso-parametric line lines don’t reflect the bump in the surface, which is however emphasized by the focal analysis on the bottom right.

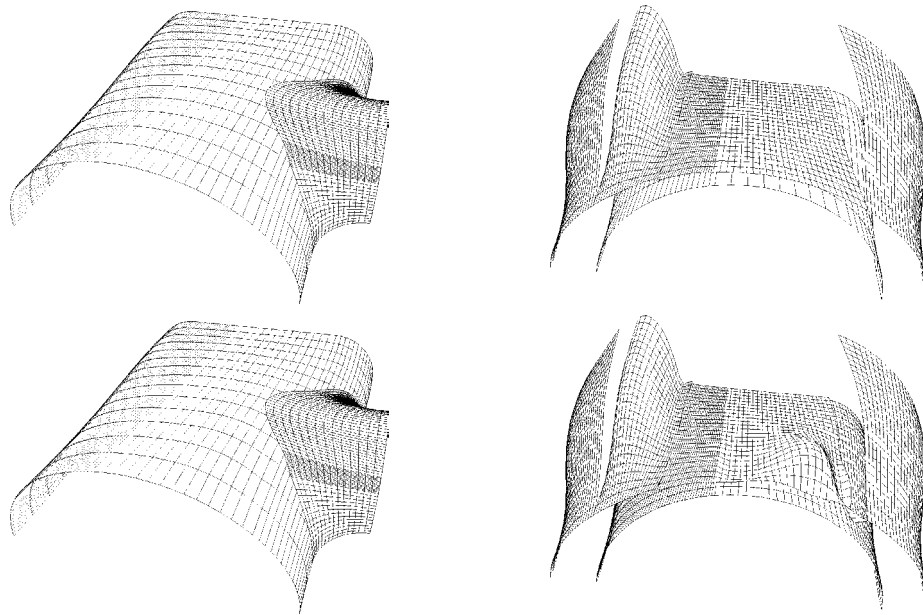


Figure 18: *Hair dryer: fairness test*

3.4 Detection of inflections

The polarity method and the orthotomics are both interactive interrogations tool, which only detect one surface “imperfection”: the change of the sign in the Gaussian curvature.

Surface with only convex iso-parameter lines are not necessarily convex in the sense that their Gaussian curvature not needs to be positive at all surface points. Such surface imperfections can not always be seen and need a special analysis: color maps, generalized focal surfaces or the following two methods can do this.

3.4.1 Orthotomics

If we start with a surface $X(u, w)$ and a point P , which is not on X and which does not lie on any tangent plane of X , P is reflected by a tangent plane of X and we multiply this length by a factor k . The parameter form of the k -orthotomic surface of X with respect to P is

$$Y_k(u, w) = P + k \left((X(u, w) - P) \cdot N(u, w) \right) N(u, w),$$

where $N(u, w)$ is the unit normal vector of the surface.

The following fact is important for applications [23]:

Let $X(u, w)$ be a regular surface and let P be a point not on the surface or on any tangential plane of the surface. The k -orthotomic surface $Y_k(u, w)$ of $X(u, w)$ with respect to P has a singularity in (u_0, w_0) , if and only if the Gaussian curvature of X vanishes, or changes its sign at this point.

To illustrate this method we consider a Bézier surface with completely convex parameter lines, shown in Fig. 19a. But this surface is not convex: As Fig. 19b shows, the orthotomic analysis emphasizes the change of sign of the Gaussian curvature in the corner region.

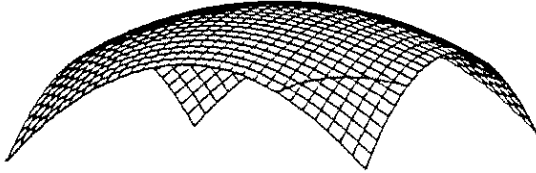


Figure 19a: *Bicubic surface patch*

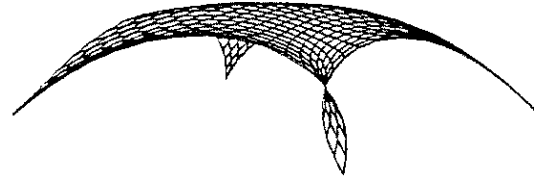


Figure 19b: *Orthotomic analysis*

3.4.2 Polarity method

The polarity method is an interactive method able to detect unwanted changes in the sign of the Gaussian curvature. For curves it detects inflection points. It uses the polar image of a curve or surface, where the singularities (cusps, edge of regression) of this image indicate the existence of points with vanishing Gaussian curvature.

We will describe the principle of this method using a planar curve $X(t) = (x(t), y(t))$. An arbitrary point (parameter $t = t_0$) on this curve is mapped by the polarity at the unit circle onto the straight line $x(t_0) + \eta y(t_0) + 1 = 0$.

If t is varied within its definition range, the created set of straight lines envelope a polar curve $P(t)$ of $X(t)$. Differentiation and elimination lead to the parameter form of $P(t)$:

$$P(t) = \begin{bmatrix} \xi(t) \\ \eta(t) \end{bmatrix} = \begin{bmatrix} -\dot{y} \\ \frac{x\dot{y} - \dot{x}y}{x\dot{y} - \dot{x}y} \end{bmatrix}^T$$

The polar curve of a curve in $3D$ is determined in an analogue way.

In the case of a surface in parameter form $X(u, w) = (x(u, w), y(u, w), z(u, w))$ the result of a polarity at the unit sphere is a polar surface $P(u, w)$ with the parameter form:

$$P(u, w) = N \cdot \frac{\det |N, X_1, X_2|}{\det |X, X_1, X_2|} = \frac{[X_2 \times X_1]}{\det |X, X_1, X_2|}.$$

The following facts are important for applications:

- If the planar curve $X(t)$ has an inflection point for $t = t_0$, then the polar curve $P(t)$ has a singularity for $t = t_0$.
- If the surface $X(u, w)$ has a root or change of sign in the Gaussian curvature at (u_0, w_0) , then the polar surface has a singularity here.

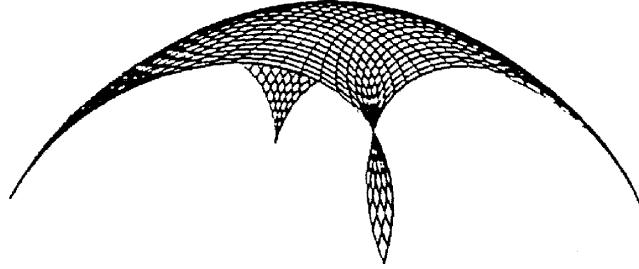


Figure 20: *Polar surface of a bicubic Bézier patch*

This polar surface looks similar to the orthotomic surface (Fig. 19b), because the center of polarity is chosen to be equal with the projection point of the orthotomic analysis (see section 3.4.1). For more informations about the polarity method and how removing the inflections, see Hoschek [24].

3.5 Color mappings

While displaying a shaded image of the surface one is free to choose a color of each surface point. *Color maps* are used to visualize functions over a surface and *texturing* can emphasize the spatial perception of an 2D image of the surface.

3.5.1 Color maps

A color-coded map is an application, which associates to a scalar function value a specific color. The color scale presents an even gradation of color corresponding to the range of function values. Colors are principally used to visualize either continuously or discontinuously any scalar function over a surface (see, for example Dill [9], Beck et al. [2], Barnhill et al. [1], Forrest [16]), like pressure, temperature, or curvature. Colors are used as a fourth dimension and show the user immediately and quantitatively how the function varies over the surface.

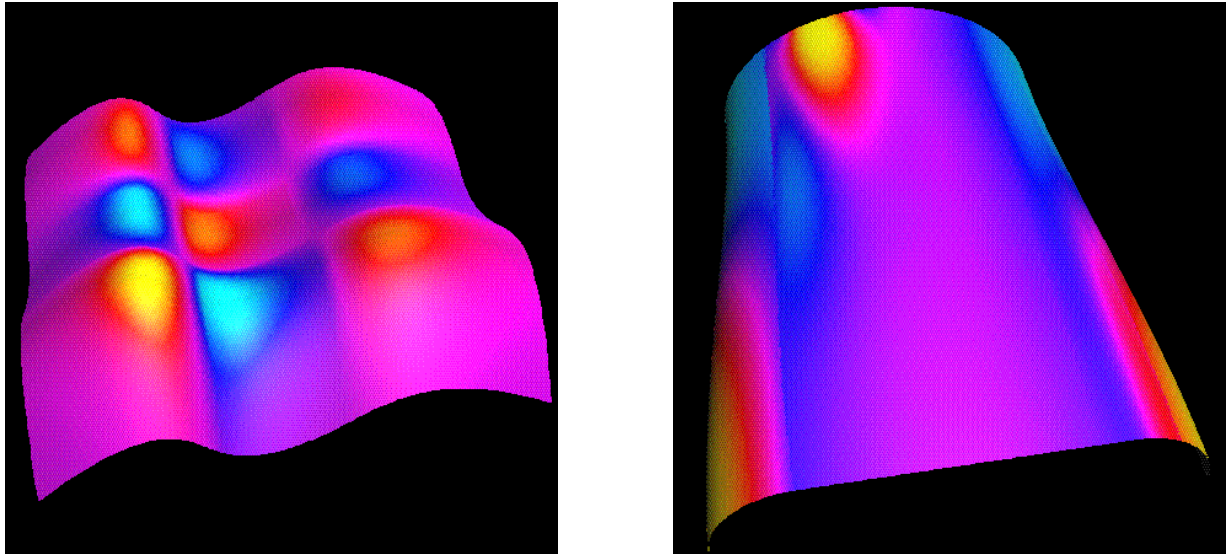


Figure 21: *Color codings of Gaussian curvature*

The Gaussian curvature map conveys information about local surface shape. It displays unwanted local behaviours as well as surface irregularities, because it is very sensitive to small changes of the Gaussian curvature, if the color is well encoded.

An even gradation of the linear or cyclic color coding is important to visualize the rapid curvature variation by the presence of color fringes. Beck et al. [2] propose to use the HSI (hue, saturation, intensity) model and to perform transformations between this space and the three primary colors RGB. See Foley et al. [15] for more details on color spaces and transformations.

An example of discrete color-coding of the interval $[0,1]$ is the following one:

<u>interval</u>	<u>Red</u>	<u>Green</u>	<u>Blue</u>	<u>Color</u>
0.0 - 0.2	1	0	0	red
0.2 - 0.4	1	1	0	yellow
0.4 - 0.6	0	1	0	green
0.6 - 0.8	0	1	1	turquoise
0.8 - 1.0	0	0	1	blue

If one is interested in the change of sign of the Gaussian curvature K for a convexity test, one might assign the color red to areas with positive Gaussian curvature, areas where K is negative are blue, and areas where it is near zero are yellow. Color maps of the maximum and minimum principal curvatures are of primary interest, when a surface is to be machined by a spherical cutter (see also section 3.3.2).

The main difficult of this simple interrogation method is the choice of a convenient color scale, which obviously is depending on the function values to be visualized.

3.5.2 Pseudo texture

The use of colors for displaying a surface helps to emphasize the 3D understanding of an 2D image by simulating shadows, perspective and depth of the object. An artificial

texturing is an aid for visualizing rendered surfaces. Isoparametric lines are commonly used, but they are in some situations ambiguous. Schweitzer [41] projects equally spaced dots of equal size over the surface in order to increase the visual perception of the form.

3.6 Characteristic lines

In this section two methods for analyzing surfaces are presented which consist of *lines of curvature* and *geodesic paths*. In each case a net of lines on the surface can be created, and should be interpreted with the knowledge of differential geometry. They are the most sophisticated tools from the mathematician's point of view. The use of these tools is nevertheless limited, because of their cumbersome calculations and their lack of intuition for interpretation of their pattern. From the practical point of view, the user should be used to interpret the lines of curvature or the geodesic paths, otherwise he won't have any profit. Numerous graphical examples are illustrated in Porteous [38], Farouki [12].

3.6.1 Lines of curvature, umbilics

Lines of curvature are curves whose tangent directions coincide with those of the principal directions, which are orthogonal. They form therefore an orthogonal net on the surface.

The net of lines of curvature becomes singular at an umbilical point where κ_1 and κ_2 are identical and the principal directions are indeterminate. Some numerical integration method is used to calculate the lines of curvature. But the integration process becomes unstable near an umbilic. Unfortunately umbilics appear frequently on free form surfaces. A recent work about umbilics (Maekawa, Wolter, Patrikalakis [32]), destinate for use in CAGD*, presents a procedure to compute the lines of curvature near an umbilic. And in Maekawa, Patrikalakis [31] a computational method to locate all isolated umbilics on parametric polynomial surfaces is described.

However, umbilics and lines of curvature figure in classical differential geometry literature, like Darboux [8], or in a more recent book of Porteous [38]. We don't want to extend this aspect here and are now focusing on the computation of lines of curvature.

Every principal curvature direction vector must fulfill equation (2.7). Solving the first equation of (2.7) we get

$$\begin{aligned} \dot{u} &= \frac{du}{ds} = \alpha(h_{12} + \kappa g_{12}) \\ \dot{w} &= \frac{dw}{ds} = -\alpha(h_{11} + \kappa g_{11}), \end{aligned} \tag{6.1}$$

where α is an arbitrary non-zero factor. Since the principal direction vector must also satisfy the second equation of (2.7), we get

$$\begin{aligned} \dot{u} &= \frac{du}{ds} = \beta(h_{22} + \kappa g_{22}) \\ \dot{w} &= \frac{dw}{ds} = -\beta(h_{12} + \kappa g_{12}). \end{aligned} \tag{6.2}$$

* CAGD: Computer Aided Geometric Design

The solutions \dot{u} and \dot{w} of (6.1) and (6.2) are linearly dependent, because the system of linear equations given by (2.7) has a rank loss than 2.

It remains to calculate α and β . We eliminate these factors by adopting arc-length s to parameterize the curvature line and by using the normalization condition

$$g_{11} \left(\frac{du}{ds} \right)^2 + 2g_{12} \left(\frac{du}{ds} \right) \left(\frac{dw}{ds} \right) + g_{22} \left(\frac{dw}{ds} \right)^2 = 1. \quad (6.3)$$

Substituting (6.1) and (6.2) respectively, into (6.3) gives the factors

$$\alpha = \frac{\pm 1}{\sqrt{g_{11}(h_{12} + \kappa g_{12})^2 - 2g_{12}(h_{12} + \kappa g_{12})(h_{11} + \kappa g_{11}) + g_{22}(h_{11} + \kappa g_{11})^2}} \quad (6.4)$$

$$\beta = \frac{\pm 1}{\sqrt{g_{11}(h_{22} + \kappa g_{22})^2 - 2g_{12}(h_{22} + \kappa g_{22})(h_{12} + \kappa g_{12}) + g_{22}(h_{12} + \kappa g_{12})^2}}, \quad (6.5)$$

where κ represents either of the two principal curvatures κ_1, κ_2 .

To solve these two coupled, non-linear differential equations (6.1) or alternatively (6.2) (the solutions obtained from (6.1) and (6.2) are linearly dependent), a numerical integration method for initial value problems must be used: constant-step fourth-order *Runge-Kutta method* or multi-step *predictor-corrector methods*, like Adams methods [Strang42]. The initial conditions are the coordinates (u, w) of a start point, since at each point the lines of curvature are unique.

Some practical hints for using such a method when integration across a multipatch surface is given in Beck et al. [2]. Maekawa et al. [32] explain in more detail the appropriate choice of the sign of α and β . They also point out that in some special situations it is preferable to solve either equation (6.1) or (6.2).

3.6.2 Geodesic paths

Geodesic paths are lines which connect two points on a curved surface with minimum path length. A lot of practical applications related to optimal path finding make use of geodesic paths, for example optimal motion planning on a curved surface for robot programming. The study of geodesics is a rather complex concern and needs a lot of more theoretical and numerical attention as the following overview can provide (for a rigorous treatment of geodesics see for example Kreyszig [29], Eisenhart [11]).

A general parametric curve (path) $C = C(t) = (u(t), w(t))$ on the surface X is given by $\bar{X}(t) = X(u(t), w(t))$. The length of this surface path between two points with parameter values t_0 and t_1 is then obtained by integration of the line element (called distance element) (2.3)

$$s = \int_{t_0}^{t_1} \sqrt{\dot{\bar{X}}^2} dt = \int_{t_0}^{t_1} \sqrt{g_{11}\dot{u}^2 + 2g_{12}\dot{u}\dot{w} + g_{22}\dot{w}^2} dt. \quad (6.6)$$

We now introduce a perturbation of this path by

$$\begin{aligned} \tilde{u}(t) &= u(t) + \varepsilon p(t) \\ \tilde{w}(t) &= w(t) + \varepsilon q(t), \end{aligned} \quad (6.7)$$

where ε is a small parameter, and we are interested in the change in s . p and q must satisfy the end conditions $p(0) = p(1) = q(0) = q(1) = 0$. We need to find at the end the path which causes the distance to attain extreme values. To do so we substitute the path (6.7) in equation (6.6) and keep only the terms which are of first order in ε . Setting then $ds/d\varepsilon = 0$ for extreme path length, we get the Euler equations:

$$\begin{aligned}\frac{d}{dt} \frac{\partial \Phi}{\partial \dot{u}} - \frac{\partial \Phi}{\partial u} &= 0 \\ \frac{d}{dt} \frac{\partial \Phi}{\partial \dot{w}} - \frac{\partial \Phi}{\partial w} &= 0,\end{aligned}\tag{6.8}$$

where $\Phi(u, w, \dot{u}, \dot{w}) = \sqrt{g_{11}\dot{u}^2 + 2g_{12}\dot{u}\dot{w} + g_{22}\dot{w}^2} dt$. This are the *geodesic differential equations*, which have to be satisfied by geodesic paths.

To bring them in a more convenient form for numerical computations, one chooses arc-length s for the parameter variable t and gets by use of equation (2.3) the following equations:

$$\begin{aligned}\frac{d^2 u}{ds^2} + \Gamma_{11}^1 \left(\frac{du}{ds}\right)^2 + 2\Gamma_{12}^1 \left(\frac{du}{ds}\right) \left(\frac{dw}{ds}\right) + \Gamma_{22}^1 \left(\frac{dw}{ds}\right)^2 &= 0 \\ \frac{d^2 w}{ds^2} + \Gamma_{11}^2 \left(\frac{du}{ds}\right)^2 + 2\Gamma_{12}^2 \left(\frac{du}{ds}\right) \left(\frac{dw}{ds}\right) + \Gamma_{22}^2 \left(\frac{dw}{ds}\right)^2 &= 0,\end{aligned}\tag{6.9}$$

where Γ_{ij}^k ($i, j, k = 1, 2$) are the *Christoffel symbols* of second kind:

$$\Gamma_{ij}^1 = \frac{N \cdot [X_{ij} \times X_2]}{\|[X_1 \times X_2]\|}, \quad \Gamma_{ij}^2 = \frac{N \cdot [X_1 \times X_{ij}]}{\|[X_1 \times X_2]\|}.$$

A curve on the surface $X(u, w)$, which satisfies these two second order differential equations is a geodesic. A geodesic path is uniquely determined by a starting point (u, w) and a direction $(du/ds, dw/ds)$ satisfying equation (6.3).

For numerical purposes it is recommended to transform equation (6.9) into 4 first order equations in 4 variables (u, w, u', w') :

$$\begin{aligned}\frac{du}{ds} &= u' \\ \frac{dw}{ds} &= w' \\ \frac{du'}{ds} &= -\Gamma_{11}^1 u'^2 - 2\Gamma_{12}^1 u'w' - \Gamma_{22}^1 w'^2 \\ \frac{dw'}{ds} &= -\Gamma_{11}^2 u'^2 - 2\Gamma_{12}^2 u'w' - \Gamma_{22}^2 w'^2.\end{aligned}\tag{6.10}$$

An appropriate Runge-Kutta method can be applied for numerical integration. The algorithm provides a method to perform initial value integrations of geodesic paths, i.e. an initial value and a start direction must be given. It is numerically more difficult to perform boundary-value integration, i.e. the specification of geodesic paths between two given points on the surface. A solution for that problem can be found in Farouki [12].

4 References

1. **Barnhill, R; Farin, G; Fayard, L; Hagen, H:** Twists, curvature and surface interrogation, *CAD* **20**, 314–346, (1988)
2. **Beck, James; Farouki, Rida; Hinds, John:** Surface analysis methods, *IEEE CG & Appl.* **6**, 19–35, (1986)
3. **Beier, Klaus-Peter:** The porcupine technique: principles, applications, and algorithms, Technical Report, University of Michigan, October (1987)
4. **Beier, Klaus-Peter; Chen, Yifan:** Highlight-line algorithm for realtime surface quality assessment, *CAD* **26**(4), 268–277, (1994)
5. **Böhm, W:** *Differential geometry of curves and surfaces*, in [13????]
6. **Böhm, W; Farin, G; Kahmann, ?:** Survey on curves and surfaces ???? *CAGD* **1**. 1–60, (1984)
7. **Brady, M; Ponce, J; Yuille, A; Asada H:** Describing surfaces, *Computer Vision, Graph. and Image Proc.* **32** 1–28, (1985)
8. **Darboux, G:** *Leçons sur la théorie générale des surfaces, Tome 4*, Gauthier-Villars, Paris, (1896)
9. **Dill, John:** An application of color graphics to the display of surface curvature, *Computer Graphics*, **15**(3), 153–161, (1981)
10. **do Carmo, P.M:** *Differential geometry of curves and surfaces*, Prentice-Hall, Englewood Cliffs, (1976)
11. **Eisenhart, L.P:** *An introduction to differential geometry*, Princeton University Press, Princeton, N.J., (1976)
12. **Farouki, R.T:** Graphical methods for surface differential geometry, in *Mathematics of surfaces*, R. Martin (ed.), IMA Series, 363–385, (1987)
13. **Farin, Gerald:** *Curves and surfaces for computer aided geometric design*, Academic Press, (1988)
14. **Farin, Gerald; Sapidis, Nikolas:** Curvature and the fairness of curves and surfaces, *IEEE CG & Appl.* **9**, 52–57, (1989)
15. **Foley, J.D; van Dam, A; Feiner, S.K; Hughes, J.F:** *Computer Graphics. Principles and Practice*, 2nd edition, Adison-Wesley, (1990)
16. **Forrest, AR:** On the rendering of surfaces, *Computer Graphics*, 253–259, (1979)
17. **Hagen, Hans; Hahmann, Stefanie:** Generalized focal surfaces : A new method for surface interrogation, *Proceedings Visualization'92*, Boston, 70–76, (1992)
18. **Hagen, H; Hahmann, S; Schreiber, T; Nakajima, Y; Wördenweber, B; Hollemann, P:** Surface interrogation algorithms, *IEEE CG & Appl.* **12**(5), 53–60, (1992)
19. **Hagen, H; Hahmann, S; Schreiber, T:** Visualization of curvature behavior of free-form curves and surfaces, *CAD* **27**, 545–552, (1995)
20. **Hartwig, R; Nowacki, Horst:** Isolinien und Schnitte in Coonschen Flächen, in: *Geometrisches Modellieren*, Informatik Fachberichte der GI **65**, 329–343, (1982)
21. **Higashi, M; Kushimoto, T; Hosaka, M:** On formulation and display for visualizing features and evaluating quality of free-form surfaces, *Proc. Eurographics'89*, 299–309, (1989)
22. **Hilbert, David; Cohn-Vossen, S:** *Geometry and the imagination*, Chelsea Publishing Company, New York, (1952)

23. **Hoschek, Josef:** Detecting regions with undesirable curvature, *CAGD* **1**, 183–192, (1984)
24. **Hoschek, Josef:** Smoothing of curves and surfaces, *CAGD* **2**, 97–105, (1985)
25. **Hoschek, Joseph; Lasser, Dieter:** *Fundamentals of computer aided geometric design*, (1992)
26. **Kaufmann, E; Klass, R:** Smoothing surfaces using reflection lines for families of splines, *CAD* **20**, 312–316, (1988)
27. **Kjellander, Johan:** Smoothing of bicubic parametric surfaces, *CAD*, **15**, 288–293, (1983)
28. **Klass, Reinhold:** Correction of local irregularities using reflection lines, *CAD* **12**, 73–77, (1980)
29. **Kreyszig, I:** *Differential Geometry*, Univ. of Toronto Press, Toronto, (1959)
30. **Lee, R.B; Fredericks, D.A:** Intersection of parametric surfaces and a plane, *IEEE CG& Appl.* **4**(8), 48-51 (1984)
31. **Maekawa, T; Patrikalakis M:** Interrogation of differential geometry properties for design and manufacture, *Visual Computer* **10**, 216–237, (1994)
32. **Maekawa, T; Wolter F-E; Patrikalakis, N:** Umbilics and lines of curvature for shape interrogation *CAGD* **13**, 133–161, (1996)
33. **Munchmeyer, Frederick:** Shape interrogation: a case study, in Farin, G.(ed): *Geometric Modelling*, 291–301, (1987)
34. **Munchmeyer, Frederick:** On surface imperfections, in Martin, R.(ed): *Mathematics on Surfaces II*, 459–474, (1987)
35. **Nackman, L.R:** Two-dimensional critical point configuration graphs, *IEEE Trans. Pattern Analysis and machine Intelligence* **6**(4), 442–450, (1984)
36. **Petersen, CS:** Adaptive contouring of three-dimensional surfaces, *CAGD* **1**, 61–74, (1984)
37. **Poeschl, Thomas:** Detecting surface irregularities using isophotes, *CAGD* **1**, 163–168, (1984)
38. **Porteous, Ian:** *Geometric Differentiation*, Cambridge University Press (1994)
39. **Pottmann, Helmut:** Visualizing curvature discontinuities of free-form surfaces, *Proc. Eurographics'89*, 529–536, (1989)
40. **Scatterfield, S.G; Rogers, D.F:** Contour lines from a B-spline surface, *IEEE CG & Appl.* **5**(4), 71–75 (1985)
41. **Schweitzer, Dino:** Artificial texturing: an aid to surface visualization, *Computer Graphics* **17**(3), 23–29, (1983)
42. **Strang, Gilbert:** *Introduction to applied mathematics*, Wellesley-Cambridge Press (1986)